

---

## Recent Ionospheric Observations Relating to Solar-Wind--Magnetosphere Coupling [and Discussion]

M. Lockwood, M. P. Freeman, M. Saunders and R. J. Moffett

*Phil. Trans. R. Soc. Lond. A* 1989 **328**, 93-105

doi: 10.1098/rsta.1989.0026

---

### Email alerting service

Receive free email alerts when new articles cite this article - sign up in the box at the top right-hand corner of the article or click [here](#)

---

To subscribe to *Phil. Trans. R. Soc. Lond. A* go to: <http://rsta.royalsocietypublishing.org/subscriptions>

---

## Recent ionospheric observations relating to solar-wind–magnetosphere coupling

BY M. LOCKWOOD<sup>1</sup> AND M. P. FREEMAN<sup>2</sup>

<sup>1</sup>*Rutherford Appleton Laboratory, Chilton, Didcot, Oxfordshire, OX11 0QX, U.K.*

<sup>2</sup>*Blackett Laboratory, Imperial College, London SW7 2BZ, U.K.*

[Plates 1 and 2]

Simultaneous observations in the high-latitude ionosphere and in the near-Earth interplanetary medium have revealed the control exerted by the interplanetary magnetic field and the solar wind flow on field-perpendicular convection of plasma in both the ionosphere and the magnetosphere. Previous studies, using statistical surveys of data from both low-altitude polar-orbiting satellites and ground-based radars and magnetometers, have established that magnetic reconnection at the dayside magnetopause is the dominant driving mechanism for convection. More recently, ground-based data and global auroral images of higher temporal resolution have been obtained and used to study the response of the ionospheric flows to changes in the interplanetary medium. These observations show that ionospheric convection responds rapidly (within a few minutes) to both increases and decreases in the reconnection rate over a range of spatial scales, as well as revealing transient enhancements which are also thought to be related to magnetopause phenomena. Such results emphasize the potential of ground-based radars and other remote-sensing instruments for studies of the Earth's interaction with the interplanetary medium.

### 1. INTRODUCTION

It is now well established that the interplanetary medium exerts strong control over the convection of ionospheric plasma at high latitudes. This is demonstrated by a number of statistical surveys of data from satellites (Heelis 1984; Heppner & Maynard 1987), ground-based magnetometers (Friis-Christensen *et al.* 1985) and radars (Holt *et al.* 1987), which are sorted according to the speed of the solar wind flow and the orientation of the interplanetary magnetic field (IMF) embedded within it. Of particular importance is the northward component of the IMF,  $B_z$ , as predicted for convection that is driven by magnetic reconnection at the dayside magnetopause (Dungey 1961). This is most clearly demonstrated by studies of the potential across the polar cap,  $\Phi$ , derived by integrating the duskward component of the convection electric field, observed along a dawn–dusk track of a polar-orbiting satellite (Cowley 1984, 1986; Reiff & Luhmann 1986). For southward IMF ( $B_z < 0$ ),  $\Phi$  is highly anti-correlated with  $B_z$ , but for  $B_z > 0$ , a lower potential is observed which does not depend on the magnitude of  $B_z$ . Because reconnection is not expected to give positive  $\Phi$  (i.e. anti-sunward convection in the polar cap) for northward IMF, a weaker ‘viscous-like’ interaction, which also transfers momentum across the magnetopause, is often invoked. Studies which allow for the decay time of residual effects of reconnection, find that any viscous-like interactions contribute less than about 15 kV to  $\Phi$  (Wygant *et al.* 1983; see also Mozer 1984), which must be contrasted with values up to *ca.* 100 kV observed when the IMF is strongly southward.

[ 57 ]

All the above studies employed IMF and convection data that were considerably averaged. For example, direct measurements of  $\Phi$  are taken over the time that the satellite takes to traverse the polar cap (from *ca.* 10 min to 1 h, depending on altitude) and radar observations often use long (typically  $\frac{1}{2}$  h) scanning cycles to maximize latitude coverage. The use of statistical surveys further smooths the data. In addition, to fit flow streamlines (plasma equipotentials) to the averaged data it is often assumed that the pattern is in the steady state, so that the potential across the dayside merging gap (mapping to that part of the dayside magnetopause where reconnection with the IMF is occurring),  $\Phi_m$ , is equal to that across the nightside reconnection region (mapping to the neutral line in the geomagnetic tail where the Earth's field lines are closed again),  $\Phi_n$ . In the general case, the area of the ionospheric polar cap (defined here as the region of open field lines, with one end in the ionosphere and the other connected to the IMF),  $A$ , is simply governed by Faraday's law,

$$\frac{d}{dt} \int_A B_1 dA = \Phi_m - \Phi_n, \quad (1)$$

where  $B_1$  is the magnetic field (Coroniti & Kennel 1973). Hence the assumption of  $\Phi_m = \Phi_n$  ( $= \Phi$ ), gives constant  $A$ . In practice,  $\Phi_m$  varies in response to changes in solar wind speed ( $V_{sw}$ ) and  $B_z$ ,  $\Phi_n$  shows explosive increases during substorms, and  $A$  is observed to respond to such changes (Holzer *et al.* 1986). Hence, it is not expected that the assumption of a steady-state polar cap and convection pattern will be valid in anything more than an average sense and the results presented in this paper underline how misleading statistical patterns of convection can be when looking at instantaneous flow patterns.

The recent studies described here make use of remotely-sensed data from ground-based radars and magnetometers and global auroral images from satellites (none of which suffer from the spatial-temporal ambiguity problem of *in situ* satellite data) that are of unprecedented temporal resolution (a few seconds). These reveal new ionospheric convection phenomena, with important implications for the magnetopause processes that drive them.

## 2. RESPONSE OF CONVECTION TO CHANGES IN THE $B_z$ COMPONENT OF THE IMF

A variety of coupling functions combining  $V_{sw}$  and  $B_z$  have been devised to quantify role of the interplanetary medium in correlative studies with terrestrial parameters. In this section, we are concerned with the lags of the ionospheric responses and not with which function yields the best cross-correlation. All lags quoted are estimates of the period between a perturbation impinging on the dayside magnetopause and the onset of an ionospheric response, i.e. the estimated propagation time from the satellite to the magnetopause has been subtracted, with allowance for slowing at the bow shock. From ground-based magnetometer data, the auroral DP1 (disturbance polar) current system (which reflects  $\Phi_n$ ) has been shown to respond to changes in the IMF with a response time of order  $\frac{1}{2}$ –1 h (see, for example, Baker *et al.* 1983). Etemadi *et al.* (1988) have carried out an equivalent statistical survey of the dependence of convection in the dayside auroral F-region (observed at 2.5-minute resolution by the Polar experiment of the EISCAT (European incoherent scatter) radar) on the interplanetary medium (observed by the AMPTE-UKS and -IRM satellites (*Active Magnetospheric Particle Tracer Explorers U.K. Subsatellite and -Ion Release Module*), immediately sunward of the bow shock). The response time is found to be considerably shorter than for the DP1 currents, being generally

5–10 min, as shown in figure 1. Similar lags were reported for the DP2 current system (the E-region Hall current equivalent to F-region convection) as long ago as 1968 by Nishida and also for  $\Phi$  inferred from magnetometer networks (Reiff *et al.* 1985). Figure 1 shows that the response lag is a function of the MLT (magnetic local time) of the ionospheric observations, being larger at greater distances from noon.

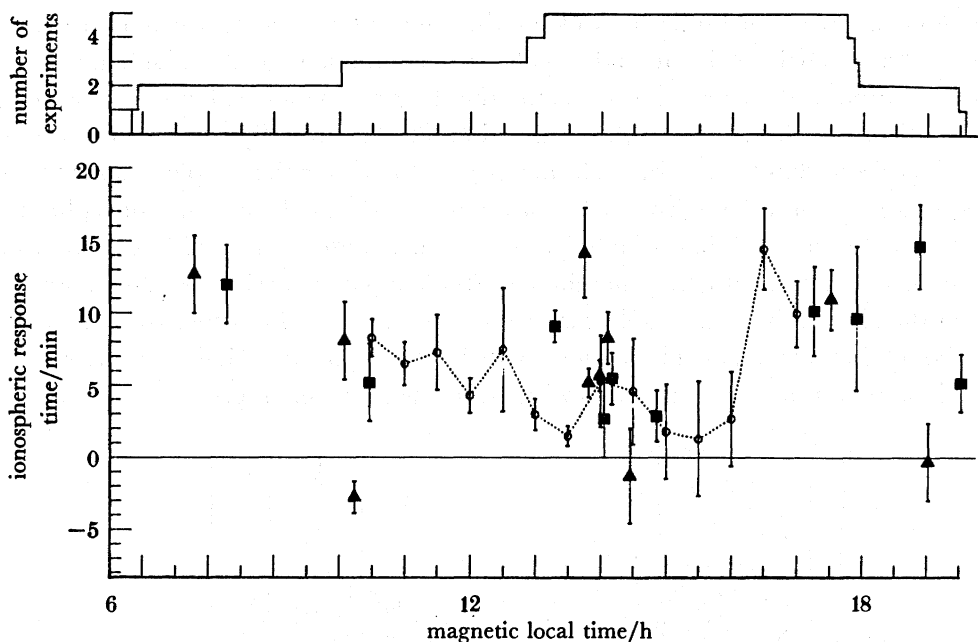


FIGURE 1. Observations of the lag of the ionospheric response to changes in the IMF from simultaneous observations by the EISCAT experiment Polar and the AMPTE-UKS and -IRM satellites. Open circles (joined by dotted line) are the results of a correlative study by Etemadi *et al.* (1988). Other data points are for case studies of flow onsets following southward (triangles) and northward (squares) turnings of the IMF by Todd *et al.* (1988*a*).

Recently, Todd *et al.* (1988*a*) have reviewed the same EISCAT-AMPTE data-set as used by Etemadi *et al.* (1988), and identified all the strong southward and northward turnings of the IMF. One of these events, which has also been studied by Rishbeth *et al.* (1985), Willis *et al.* (1986) and Lockwood *et al.* (1986*a*), is shown in figure 2, plate 1. The EISCAT vector data (bottom panel) show a marked flow enhancement near 11h20 U.T. (Universal Time), after AMPTE-UKS had observed  $B_z$  to turn negative at 11h07 U.T. (middle panel). Inspection of the 15 s line-of-sight velocities allowed Todd *et al.* to identify the onset of the appropriate ionospheric response and the lags derived for this and the other events are shown in figure 1, in addition to the results of Etemadi *et al.* It can be seen that statistical and case studies give similar values for the delay of the ionospheric response.

Holzer *et al.* (1986) have reported that the polar cap, defined by DMSP (Defense Meteorological Satellite Program) satellite observations of the poleward precipitation boundary, begins to expand in response to a southward turning of the IMF, with a lag of less than 15 min. This expansion continues for roughly an hour, when it is halted by an increase in  $\Phi_n$ , which is reflected in a strengthening of the auroral electrojet, commencing 30 min after the start of the cap expansion.

These observed ionospheric response times are rather surprising in that the perturbation is

expected to propagate from the subsolar magnetopause to the ionosphere at the field-aligned Alfvén velocity which gives a delay of only 1–2 min. Information on this would be transmitted through the ionosphere at the field-perpendicular Alfvén speed, which is so large that this should give negligible additional delay. One possible explanation of the additional delay has been put forward by Southwood (1987) and is presented schematically in figure 3. In figure 3*a*, newly-opened flux tube is pulled polewards and it is suggested that the ionospheric foot does not begin to move until the kink in the tube, at the point when it threads the magnetopause, has been ironed out and a poleward component of the magnetic field-line tension has been produced, which can overcome the drag on the ionospheric foot of the tube and move it anti-sunward. Cowley (1980) has estimated that initially the velocity of motion of the kink,  $V_t$ , is about  $250 \text{ km s}^{-1}$  for a plasma of  $\beta \approx 1$  and, for the simple geometry shown in figure 3*a*, this must move roughly  $12 R_E$  ( $R_E = 6.37 \times 10^6 \text{ m}$ ) before the ionospheric foot of the tube begins to move, giving a lag of some 5 min. In figure 3*b*, a different situation is described where magnetosheath flow dominates over magnetic tension and/or a strong  $B_y$  component of the IMF results in a largely east–west motion of the flux tube. In such cases the ionospheric foot of the tube may begin to move with a delay of just the Alfvén propagation time (1–2 min). These two different situations will be discussed further in §5.

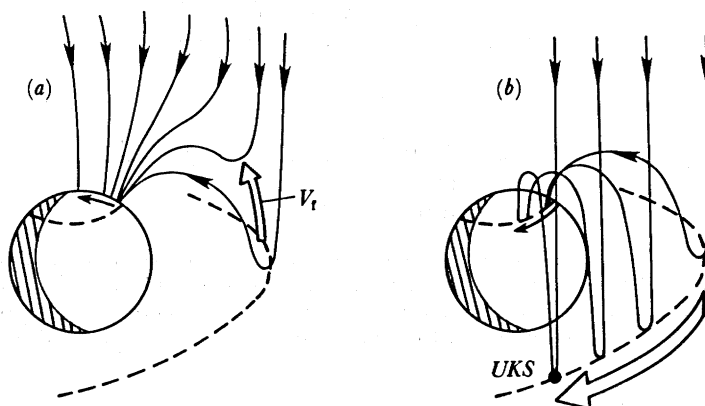


FIGURE 3. Schematic of the evolution of a newly connected flux tube for cases where the join of magnetospheric and magnetosheath arms moves (a) poleward under the influence of magnetic tension at speed  $V_t$  and (b) towards dusk or, as shown here, dawn under the influence of magnetosheath flow. The point shown is where ionospheric ions in the wake of a flux transfer event (FTE) have been reported from UKS observations (Lockwood *et al.* 1988*b*).

Clauer & Friis-Christensen (1988) have reported observations of a northward turning of the IMF, which caused a rotation from anti-sunward to sunward flow in the polar cap, inferred from the Greenland magnetometer network. The rotation commences after a lag of just 3 min (i.e. an Alfvén wave propagation time to within the error due to the estimation of the satellite to magnetopause transit time), but is not completed for another 22 min. Hence it would appear that reconnection at the edges of the lobes during periods of strong northward IMF, unlike that at the subsolar magnetopause, immediately exerts a force on the ionospheric foot of the newly opened flux tube. This may be consistent with field-line tension and the geometry of the merging flux tubes, there being no kink to straighten in this case. The establishment of a pattern of sunward convection in the polar cap has also recently been deduced using the global, auroral ultraviolet (UV) imager on the *Viking* satellite (Murphree *et al.* 1989*a*). During a sequence of 1 min resolution images, the IMF was consistently northward and a convection



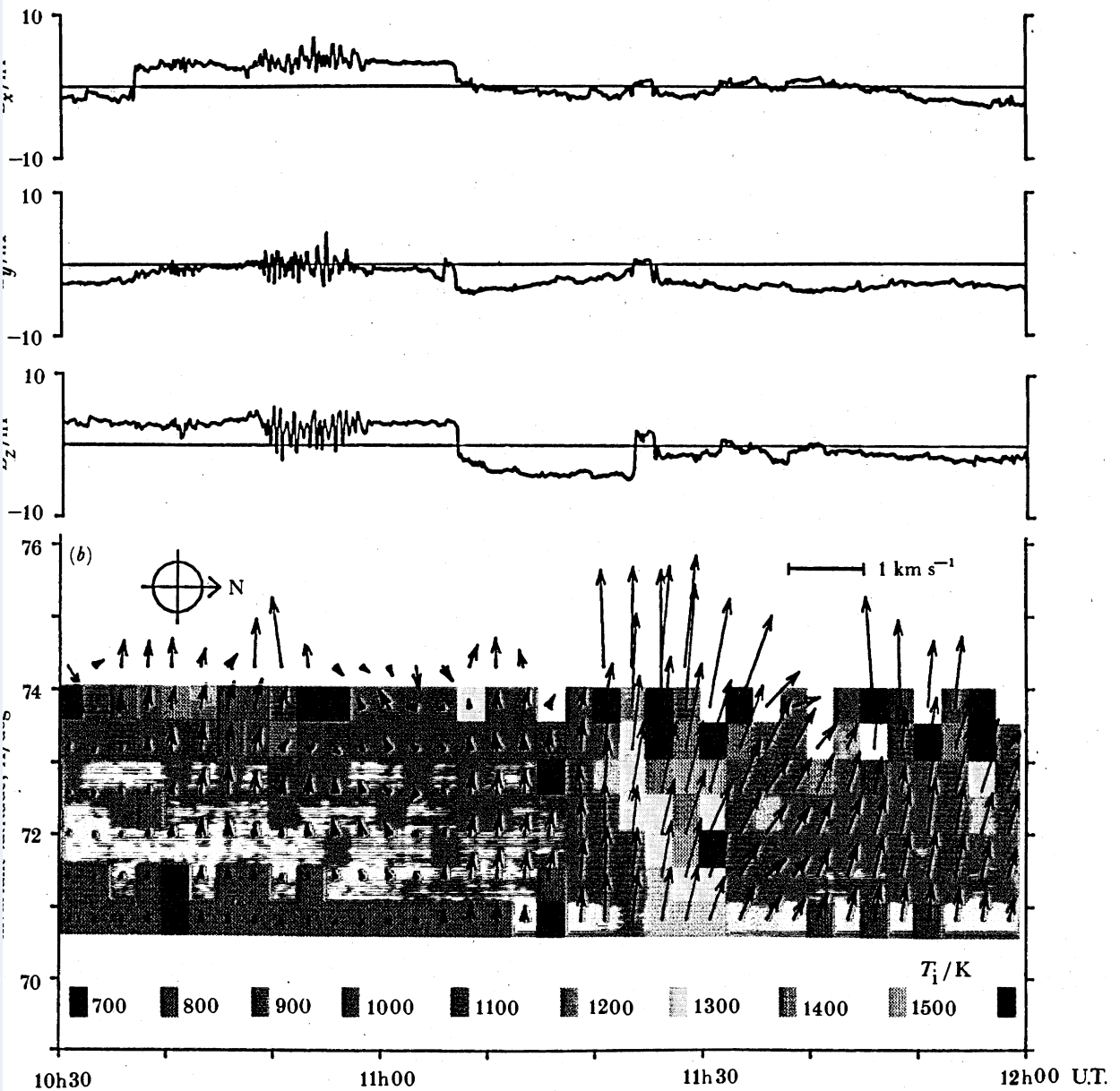


FIGURE 2. Example of an observed ionospheric response to a southward turning of the IMF (27 October 1984). (a) The sunward, dawnward and northward components of the IMF in GSM coordinates ( $B_x$ ,  $B_y$  and  $B_z$ , respectively), observed by AMPTE-UKS when located immediately sunward of the Earth's bow shock. (b) The simultaneous observations by the EISCAT radar. The flow vectors have been rotated through  $90^\circ$  to avoid congestion of the plot; hence northward flow is shown by vectors directed to the right of the figure and westward flow by vectors directed upward (i.e. the vectors are in the direction of the electric field). The vectors are superimposed on a colour plot of two-minute averages of the ion temperature,  $T_i$ . (From Willis *et al.* 1986.)

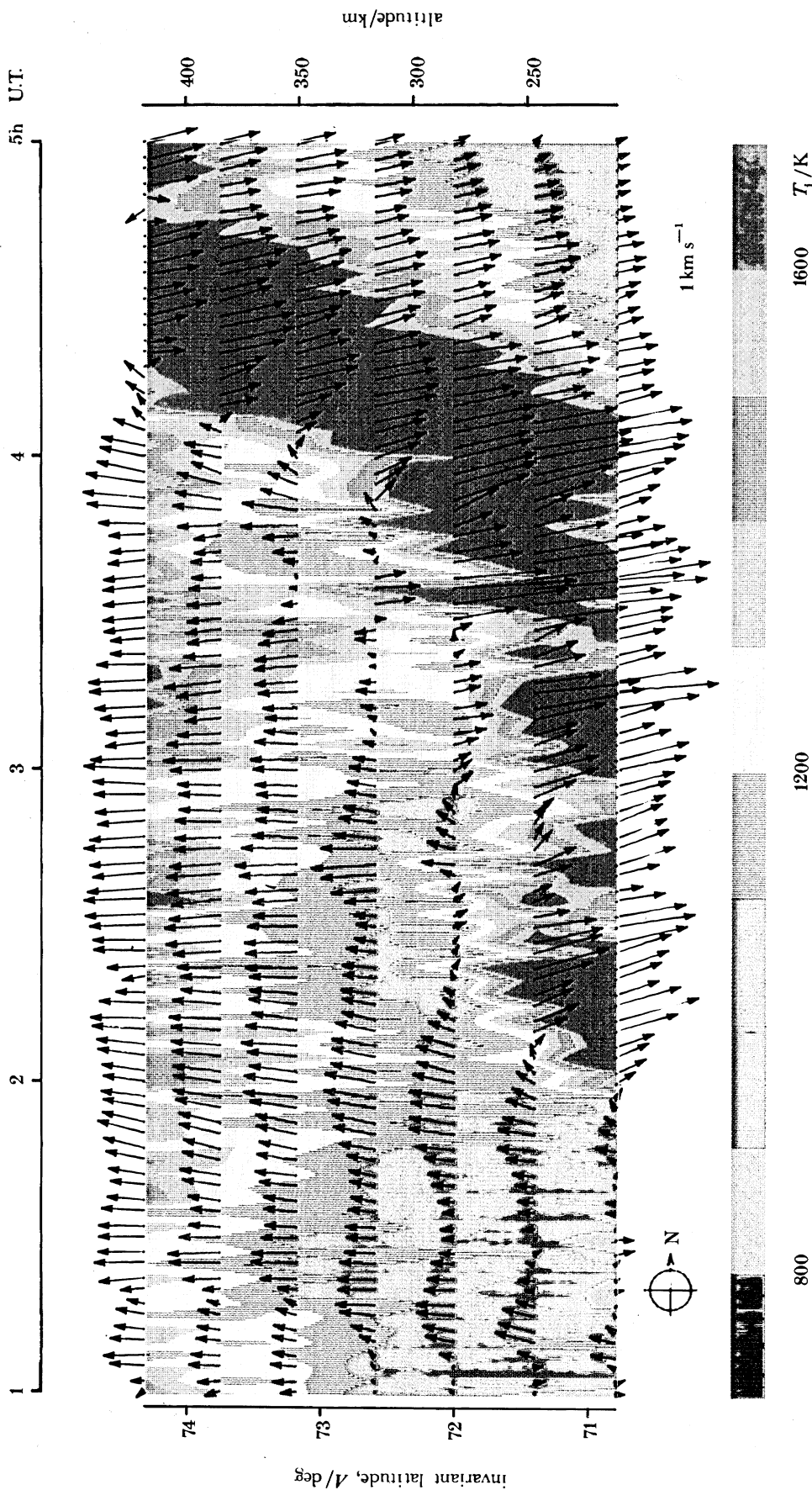


FIGURE 5. EISCAT observations of the polar cap boundary near dawn showing a polar cap contraction and evidence for viscous-like interaction across the magnetopause. The data presentation format is the same as that used in figure 2. A band of high ion temperature is seen immediately equatorward of the boundary which appears as a rotational reversal of the flow vectors from westward to eastward, through northward, and moves rapidly poleward across the field-of-view between 03h45 and 04h15 U.T.

change was triggered by a change in sense of IMF  $B_x$ . The effect of the  $B_x$  component of the IMF is often neglected, but for positive  $B_x$  it can determine in which of the two polar caps, if not both, sunward convection occurs (Reiff 1982). The initial response (1–2 min after the change in  $B_x$ ) was the formation of a spot of high luminosity, poleward of the cusp aurora. This ‘bright spot’ indicates that merging has begun on the edge of the lobe in the observed hemisphere. Subsequently, a sun-aligned arc (also called ‘theta aurora’) grows from the nightside oval, sunward over the polar cap, reaching the bright spot some 10 min later. This can be interpreted as flux tubes, containing plasma-sheet plasma, moving through the centre of the lobe towards the new merging region, thereby bifurcating the lobe.

### 3. INFLATION AND DEFLATION OF THE POLAR CAP

The events studied by Todd *et al.* (1988a) include examples of northward turnings of the IMF which cause major decreases in the flows observed by EISCAT, with the delays discussed above. In the event described by Clauer & Friis-Christensen (1988), the flows observed by the Sondre Stromfjord radar (equatorward of the region where sunward convection grows) are also observed to slow near the time of the northward turning. These results are somewhat surprising as, following a northward turning, the remaining open field lines in the polar cap might be expected to continue to drive convection, and hence the ionospheric flows should decrease with the long timescales required to reduce  $A$ , deduced by using realistic values for  $A$  and  $\Phi_n$ . In addition, the thermospheric winds driven by strong convection are slowed on a timescale of tens of minutes and should act to maintain convection following a northward turning, the so-called ‘flywheel’ effect. The winds are not sufficiently strong in most regions to maintain more than a low level of convection which would decay gradually following the initial slowings when the IMF turns northward. The observations given by Todd *et al.* (1988a) show that, after an initial slowing 5–10 min following a northward turning at the magnetopause (to a speed rather greater than predicted by the neutral wind flywheel), there is a more gradual slowing. In considering this behaviour, it is important to include the effects of  $dA/dt$  on the convection pattern. In this section we discuss how the rate of change of cap area can help to explain both the initial responses to northward turnings and the short response lags of auroral flows to  $B_x$  changes of either sense, as described in §2.

Siscoe & Huang (1985) considered the convection pattern for an applied  $\Phi_m$  with  $\Phi_n = 0$ . Outside the merging gap, across which  $\Phi_m$  is applied, the polar cap boundary is ‘adiarocic’ (meaning ‘not flowing across’), and hence the boundary moves with the plasma as the polar cap inflates according to equation (1). If the boundary is assumed to remain circular (which at least from global auroral images would appear to be valid except during substorms), the potential is distributed evenly around the expanding boundary, and return flow on auroral field lines is entirely driven by the expanding polar cap pushing closed field lines out of the way (the largely incompressible nature of the ionosphere allows such simple hydrodynamic concepts to be used). Figure 4a is a schematic of the flow pattern, similar to that described by Siscoe & Huang (1985), but with the addition of a non-zero nightside reconnection potential,  $\Phi_n$ . In this example,  $\Phi_m$  is twice  $\Phi_n$  and hence the cap is inflating. Note that half the return flow on the dayside is driven by tail reconnection and half by the equatorward-moving adiarocic boundaries. In figure 4b, we have considered the same  $\Phi_n$  but reduced  $\Phi_m$  by a factor of 4 to simulate the effect of a northward turning of the IMF. Now the cap is contracting at half the rate



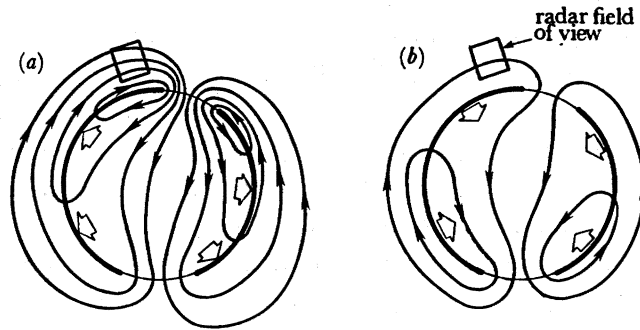


FIGURE 4. Schematic of ion convection patterns for an (a) inflating and (b) deflating polar cap. (a)  $\Phi_m = 2\Phi_n$ . (b)  $\Phi_m = \frac{1}{2}\Phi_n$ .

with which it was expanding in (a). The poleward-moving adiaroic boundaries give a very different convection pattern and the flow speed in the radar field of view shown (proportional to the separation of equipotentials) has fallen drastically. This will occur on closed field lines as soon as the cap ceases to expand and begins to contract. Hence it is the time derivative of  $A$  which controls the initial response of convection on closed auroral field lines. Todd *et al.* (1988a) note that the response of the observed convection also depends on the location of the field-of-view, relative to the polar cap, and hence on  $A$ , as would be predicted from figure 3. For a short period (*ca.* 5 min) after a northward turning has impinged upon the magnetopause, there may be flux tubes which are connected to the IMF, but have yet to straighten and impart momentum to the ionospheric plasma (figure 3a). Only after this time will the flows across the merging gap slow and hence  $\Phi_m$  fall. Hence this effect would give similar lags for the onset of northward and southward turnings as observed in figure 1. The rapid fall in  $\Phi_m$  also indicates that 'old' open flux tubes impart less momentum to the ionospheric plasma than do those which have been merged more recently with the IMF.

Figure 4 presents a rather different view to that taken, for example, by Coroniti & Kennel (1973) who consider that the convection response time is that for  $\Phi_n$  to adjust to the change in  $\Phi_m$ , giving the longer lags appropriate to the DP1 current system changes. Figure 4 predicts that  $\Phi_m$  exerts a more immediate and stronger control on ionospheric convection on the dayside, as is found in the recent radar data. The nightside flows are more constant in figure 4, simply because  $\Phi_n$  has been considered as constant.

Examples of polar cap expansions have recently been reported by Lockwood *et al.* (1986a) and de la Beaujardiere *et al.* (1987). In the first example, the cap boundary is observed by the Sondre Stromfjord and EISCAT radars and the *Dynamics Explorer 1 (DE1)* satellite at three different MLTs simultaneously. The results are consistent with expansion of a circular cap, resulting from a very large increase in  $\Phi_m$  (150–200 kV). The boundary observed at Sondre Stromfjord in the afternoon sector is adiaroic (i.e. flow velocity equals boundary velocity). In the example presented by de la Beaujardiere *et al.* the IMF is observed to turn southward shortly before the cap boundary begins to move equatorward. The boundary is only observed by the Sondre Stromfjord radar, at roughly the same MLT as in the previous example. In this second case, the boundary is certainly not adiaroic at Sondre Stromfjord, with northward convection across the southward-moving boundary. The difference between these days must be attributed to the variable width of the merging gap, as also recently involved to explain convection data

from the *DE2* satellite (Moses *et al.* 1988). EISCAT observations of the cap boundary during polar-cap deflation are presented in figure 5, plate 2 (after Lockwood *et al.* 1988*a*) and will be discussed further in §6.

#### 4. DISTORTIONS OF THE POLAR CAP

One of the events in the set discussed by Todd *et al.* (1988*a*) is the large step-function decrease in  $B_z$  and dramatic flow enhancement reported by Rishbeth *et al.* (1985) and Willis *et al.* (1986) and which is shown in figure 2. This southward turning has also been studied at high time resolution by Lockwood *et al.* (1986*b*), who determined that the resulting ionospheric ion temperature enhancement (which can be seen in the colour contours at the bottom of figure 2) was moving almost eastward across the field-of-view in the afternoon MLT sector. As a result, these authors suggested the growth of a region of newly opened flux, appended to the dayside edge of the polar cap, and the flow equipotentials subsequently expanding across the field of view. This picture provides a possible explanation of the increase in lag time with distance from the merging region, as reported in figure 1. The dayside cusp is known to move rapidly southward in response to a southward turning of the IMF (Burch 1973) and the location of the dayside equatorial magnetopause is observed to move earthward (Holzer & Slavin 1979). This process is called magnetospheric erosion and arises because the inflow rate to the reconnection neutral line (in a frame of reference fixed with respect to the Earth) from the magnetosheath is not balanced by that of closed field lines from the magnetosphere, so the neutral line moves earthward. The ionospheric signature of such an event has been discussed by Freeman & Southwood (1988), and used to explain data from the SABRE (Sweden and Britain Radar Auroral Experiment) radar during an erosion event (Freeman *et al.* 1989). The spatial patterns of the observed ionospheric flows show the effects of an extrusion growing on the dayside polar cap, and the subsequent decay back towards the original polar cap boundary as the merging rate decreases again.

The distortion of the polar cap described here seems to be at variance with the polar-cap inflation predicted in the §3. In both cases the growth of the area of open flux tubes is controlled by equation (1), but equatorward expansion of the boundary at MLT away from the merging gap in an isotropic expansion will give very different convection patterns to those seen in erosion events, where the growth is largely confined to the merging gap and convection pattern changes are initially much more localized. The observations described in these two sections imply both isotropic expansion of the cap and its distortion by erosion can take place. This will partly depend on the time when the southward turning arrives at the magnetopause. If it is just before a substorm, the open field lines in the geomagnetic tail will be stressed and the sunward return flow weak, allowing the dayside magnetopause to erode. Conversely, if it is just after a substorm, the release of this stress in the tail by the substorm will drive stronger sunward flow and give a larger inflow rate of magnetospheric flux into the dayside neutral line. Consequently, the dayside neutral line will not move earthward so rapidly, if at all. Even while erosion is occurring there may be cancelling  $B_y$  effects (Freeman & Lockwood 1989), as is demonstrated in figure 6. In this simple illustrative model, the shape of the cap boundary extrusion in the ionosphere is numerically calculated as a function of time for fixed merging and convection rates in the ionosphere, where newly opened flux tubes are all moved in the same direction (in part determined by the  $B_y$  component of the IMF) and at the same speed. Figure 6*a*

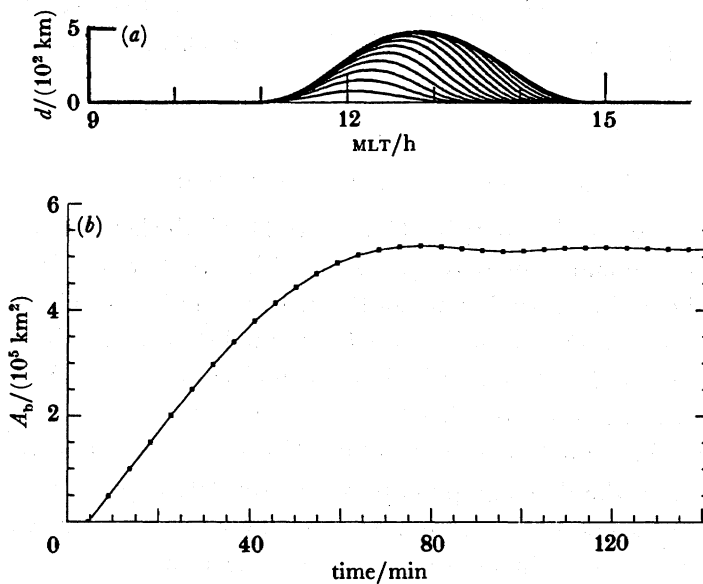


FIGURE 6. Simple model of the evolution of the ionospheric polar cap extrusion during erosion where all newly opened flux tubes are moved at  $0.8 \text{ km s}^{-1}$  in a direction at  $30^\circ$  to the east of the Sun–Earth line and the ionospheric projection of the reconnection neutral line moves equatorward at  $1 \text{ km s}^{-1}$ . In (a), the location of the open-closed field-line boundary is shown at time intervals of 4.5 min and in (b) the area of the extrusion,  $A_b$ , is plotted as a function of time.

shows that the extrusion to the boundary grows, and also propagates eastward in this example which simulates negative  $B_y$  conditions. Figure 6b shows that after about an hour, the area of the extrusion,  $A_b$ , saturates, the exact time taken depending on the model parameters used. A form of the flux conservation equation (1), appropriate to this bulge, can now be applied to examine what appears as a merging gap, of increasing width, to the old polar cap. The application of an additional dayside potential  $\Delta\Phi_m$  will increase the potential across this effective merging gap, but only by a value of  $(\Delta\Phi_m - B_1 dA_b/dt)$ . Figure 6b shows that the second term falls to zero as the bulge saturates, and then the full increase in potential is applied to the polar cap. There is no reason to expect the additional potential across this effective merging gap to be applied unevenly over the remaining polar-cap boundary, which thus should expand uniformly, and give a convection pattern of the kind shown in figure 4a. Hence we predict that an increase in  $\Phi_m$  will, in general, cause the local convection changes associated with the extrusion and at the same time cause enhancement of the whole dayside pattern, in the manner shown in figure 4. The initial balance between these two will depend on how fast, if at all, the dayside neutral line moves earthward. After a while, the expansion effect will dominate as the cap extrusion ceases to grow.

## 5. TRANSIENT PHENOMENA

It is known that reconnection at the dayside magnetopause can be patchy and vary with time. Consequently, short-lived transient flows over spatially restricted regions of the dayside auroral ionosphere are expected (Cowley 1984). For example, Southwood (1987) has predicted the ionospheric signature of a ‘flux transfer event’ (FTE) on the dayside magnetopause, by using a model where momentum is transferred to the ionosphere by a pair of

oppositely directed field-aligned currents on the flanks of an isolated newly reconnected flux tube. In this model of FTES, the connected flux tube diameter is considered to be of the order of  $1 R_E$  ( $R_E = 6.37 \times 10^6$  m) at the magnetopause, and yields a twin-vortex flow pattern in the ionosphere with a spatial extent of a few hundred kilometres. Observations of impulsive bursts of flow across the dayside polar-cap boundary with roughly this spatial scale have been reported by Goertz *et al.* (1985), using the STARE radar (Scandinavian twin auroral experiment). Almost simultaneous observations of reductions in ion and electron flows at the GEOS 2 satellite (which was on roughly the same field line if STARE was observing mainly closed field lines) were interpreted by these authors as indicating that the satellite was on the newly opened flux tube of an FTE, but the GEOS magnetometer could not resolve the characteristic FTE signature. Todd *et al.* (1986, 1988*b*) have reported EISCAT observations of impulsive flow bursts in the ionosphere, which they show are consistent with the twin vortex flow pattern predicted by Southwood. Sandholt *et al.* (1986) have reported spatially localized signatures in optical all-sky camera images which they too interpret in terms of FTES (see also Lockwood *et al.* 1988*b*). In all these observations, the repetition interval is roughly the 5 min which is found for FTES. The signature of FTES in ground-based magnetometer data has been considered by McHenry & Clauer (1987), who concluded that such observations are possible but would require a more closely spaced array of high time-resolution magnetometers than currently available.

Consideration of figure 2 poses the question whether or not FTE signatures should be seen simultaneously in the ionosphere and at the magnetopause. The ionospheric signature will only be formed once the foot of the field line is in motion, and moving faster than the surrounding flux tubes, be they closed or open. In figure 2*a* this does not occur until after the kink in the newly connected tube has been straightened, by which time the classic FTE signature in the boundary normal component of the magnetic field will no longer be observed. Hence, according to figure 3*a*, there must be a delay between the magnetopause and ionospheric signatures, which may be *ca.* 5 min, as in figure 1. Coupled with the highly limited probability of a newly opened flux tube moving across both the satellite and the radar field of view, this makes definitive identification of ionospheric effects of such FTES by multipoint observations very difficult. In the case suggested by Cowley (1984) and depicted in figure 3*b*, the FTE moves to 'low *X*'-'low *Z*' GSM (geocentric solar magnetospheric) coordinates on the magnetopause (the dawn or dusk flank) and its ionospheric signature moves around the polar cap boundary. Hence such FTES must pass both over a magnetopause satellite and through the field of view of a ground-based radar or magnetometer array in the same MLT quadrant, provided the polar-cap boundary remains within that field of view. In this case the delay between the magnetopause and ionospheric observations would depend upon a number of factors (including FTE velocity and the difference in the MLTs of the observations) and could be as large as 15 min. Lockwood *et al.* (1988*b*) interpret observations of ionospheric ions in the wake of an FTE, observed in the low-latitude boundary layer at low *X* and low *Z*, as evidence that such coordinated observations are possible.

The above values for the spatial scale size of FTE signatures in the ionosphere have recently been questioned by Southwood *et al.* (1988), who deduced larger signatures for a theory of FTES that invokes variations of reconnection rate, instead of the standard isolated flux tube model. Both models give the same signature in magnetometer data near the magnetopause, and ground-based observations are the most likely way of discriminating between them.



Glassmeier *et al.* (1989) and Friis-Christensen *et al.* (1988) have reported large (several thousand kilometres), travelling twin-vortices in flow deduced from ground-based magnetometer data. However, the velocity of motion of the pattern (typically  $4 \text{ km s}^{-1}$ ) is rather larger than expected for an FTE signature, and the flow in the centre of the event is not in the direction of motion of the pattern as a whole, as predicted by the Southwood (1987) FTE model. A similar event, observed by Potemra *et al.* (1989), has been detected simultaneously by the *Viking* and *AMPTE-CCE* (*Charge Composition Explorer*) satellites and ground-based magnetometers. This event is thought to be driven by oscillations in solar wind dynamic pressure, observed with the same period in flow data from the *IMP-8* satellite.

In addition to these vortical flow structures, a variety of wave bursts have been reported in the dayside auroral ionosphere, which are thought to relate to impulsive transients at the magnetopause, and possibly to FTES (Bol'shakova & Troitskaya 1982). Examples in radar data have been given by Waldock *et al.* (1988) and Todd *et al.* (1988*b*).

## 6. VISCOUS-LIKE INTERACTION

Most of the ground-based observations presented in this paper are explained in terms of reconnection-driven flows. This is not surprising because, as we discussed in the introduction, the majority of the potential which drives convection is attributed to reconnection and the weaker effects of a viscous-like interaction would tend to be masked by the reconnection-driven flows in the ionosphere much of the time. Recently, however, Lockwood *et al.* (1988*a*) have studied the polar-cap boundary in the midnight–dawn MLT sector which is shown in figure 5. This boundary, seen as a zonal flow reversal, contracted polewards across the EISCAT field of view. Careful inspection of these data reveals that the boundary is not a perfect shear reversal moving polewards, for two reasons: firstly, there is a decrease in the magnitude of the flow at the boundary, and secondly the boundary is not quite adiaroic. In fact, the poleward convection component normal to the boundary is found consistently to exceed the speed of the boundary motion (i.e. there is flow into the polar cap) and the potential deduced along the observed segment of the boundary (covering 2 h of MLT) is 7 kV. The MLT of these observations argues against low-level reconnection on the flanks of the magnetotail, which would also fail to explain the observed slowing of the flow at the boundary. The observations are more consistent with the viscous-like interaction on closed field lines, recently observed by Richardson *et al.* (1989), using data from the *ISEE-3* satellite when in the distant tail, and thought to be due to Kelvin–Helmholtz waves. The potential deduced by Lockwood *et al.* is roughly consistent with that required by theory and the statistical surveys of  $\Phi$  as a function of  $B_z$  (Cowley 1984, 1986; Reiff & Luhmann, 1986), and with the potential across the boundary layer deduced by Mozer (1984). The high time resolution of the uv-imager on the *Viking* satellite has allowed observations of 'strings of beads' of high luminosity, each showing vortical structure and lasting typically less than a minute, along the polar cap boundary during low magnetic activity; and observed features are also highly suggestive of the Kelvin–Helmholtz instability (Murphree *et al.* 1989*b*).

## 7. CONCLUSIONS

Remote-sensing observations with high temporal resolution of ionospheric currents, flows and luminosity offer a unique opportunity to study the temporal evolution of convection. The data show effects that are consistent with both large-scale quasi-steady reconnection at the magnetopause and smaller-scale transient events. The present evidence clearly demonstrates the effects of steady momentum transfer across the magnetopause, and a coherent picture of the various responses of convection is emerging. There is no evidence yet to prove definitively associations between the various transient phenomena in the ionosphere and at the magnetopause and the multipoint measurements required are fraught with difficulties. However, the value of ground-based observations to studies of magnetopause phenomena is now clearly established.

The authors are grateful to D. J. Southwood, S. W. H. Cowley and D. M. Willis for their comments on this paper. We also thank the following for valuable discussions: H. Todd, C. R. Clauer, J. S. Murphree, T. A. Potemra, G. L. Siscoe and J. A. Waldock and S. R. Crothers for the colour graphics.

## REFERENCES

- Baker, D. N., Zwickl, R. D., Bame, S. J., Hones, E. W., Jr, Tsurutani, B. T., Smith, E. J. & Akasofu, S.-I. 1983 *J. geophys. Res.* **88**, 6230–6242.
- Bol'shakova, O. V. & Troitskaya, V. A. 1982 *Geomag. Aeronaut.* **22**, 723–724.
- Burch, J. L. 1973 *Radio Sci.* **8**, 955–961.
- Clauer, C. R. & Friis-Christensen, E. 1988 *J. geophys. Res.* **93**, 2749–2757.
- Coroniti, F. V. & Kennel, C. F. 1973 *J. geophys. Res.* **78**, 2837–2851.
- Cowley, S. W. H. 1980 *Space Sci. Rev.* **26**, 217–275.
- Cowley, S. W. H. 1984 *Geophys. Monograph* no. **30**, pp. 375–378. Washington, D.C.: American Geophysical Union.
- Cowley, S. W. H. 1986 *J. Geomagn. Geoelect., Kyoto* **38**, 1223–1256.
- de la Beaujardiere, O., Evans, D. S., Kamide, Y. & Lepping, R. P. 1987 *Annls Geophys.* **5**, 519–526.
- Dungey, J. W. 1961 *Phys. Rev. Lett.* **6**, 47–48.
- Etemadi, A., Cowley, S. W. H., Lockwood, M., Bromage, B. J. I., Willis, D. M. & Lühr, H. 1988 *Planet. Space Sci.* **36**, 471–502.
- Friis-Christensen, E., Kamide, Y., Richmond, A. D. & Matsushita, S. 1985 *J. geophys. Res.* **90**, 1325–1338.
- Friis-Christensen, E., McHenry, M. A., Clauer, C. R. & Vennerstrøm, S. 1988 *Geophys. Res. Lett.* **15**, 253–256.
- Freeman, M. P. & Lockwood, M. 1989 *Planet. Space Sci.* (Submitted.)
- Freeman, M. P. & Southwood, D. J. 1988 *Planet. Space Sci.* **36**, 509–522.
- Freeman, M. P., Southwood, D. J., Waldock, J. A. & Rodger, A. S. 1989 *J. geophys. Res.* (Submitted.)
- Heelis, R. A. 1984 *J. geophys. Res.* **89**, 2873–2880.
- Heppner, J. P. & Maynard, N. C. 1987 *J. geophys. Res.* **92**, 4467–4489.
- Holt, J. M., Wand, R. H., Evans, J. V. & Oliver, W. L. 1987 *J. geophys. Res.* **92**, 203–212.
- Holzer, T. E., McPherron, R. L. & Hardy, D. A. 1986 *J. geophys. Res.* **91**, 3287–3293.
- Holzer, T. E. & Slavin, J. A. 1979 *J. geophys. Res.* **84**, 2573–2578.
- Glassmeier, K. H., Hoenisch, M. & Unteidt, J. 1989 *J. geophys. Res.* (In the press.)
- Goertz, C. K., Nielsen, E., Korth, A., Glassmeier, K. H., Haldoupis, C., Hoeg, P. & Hayward, D. 1985 *J. geophys. Res.* **90**, 4069–4078.
- Lockwood, M., Cowley, S. W. H., Todd, H., Willis, D. M. & Clauer, C. R. 1988a *Planet. Space Sci.* **36**, 1229–1253.
- Lockwood, M., van Eyken, A. P., Bromage, B. J. I., Willis, D. M. & Cowley, S. W. H. 1986a *Geophys. Res. Lett.* **13**, 72–75.
- Lockwood, M., van Eyken, A. P., Bromage, B. J. I., Waite, J. H. Jr, Moore, T. E. & Dounnik, J. R. 1986b *Adv. Space Res.* **6**(3), 93–101.
- Lockwood, M., Smith, M. F., Farrugia, C. J. & Siscoe, G. L. 1988b *J. geophys. Res.* **93**, 5641–5654.
- McHenry, M. A. & Clauer, C. R. 1987 *J. geophys. Res.* **92**, 11231–11241.
- Moses, J. J., Siscoe, G. L., Heelis, R. A. & Winningham, J. D. 1988 *J. geophys. Res.* **93**, 9785–9794.
- Mozer, F. S. 1984 *Geophys. Res. Lett.* **11**, 135–138.

- Murphree, J. S., Cogger, L. L., Elphinstone, R. D. & Rostoker, G. 1989*b* *J. geophys. Res.* (Submitted.)
- Murphree, J. S., Elphinstone, R. D., Hearn, D. & Cogger, L. L. 1989*a* *J. geophys. Res.* (In the press.)
- Nishida, A. 1968 *J. geophys. Res.* **73**, 5549–5559.
- Potemra, T. A., Zanetti, L. J., Takahashi, K., Erlandson, R. E., Lühr, H., Marklund, G. T., Block, L. P. & Lazarus, A. 1989 *J. geophys. Res.* (In the press.)
- Reiff, P. H. 1982 *J. geophys. Res.* **87**, 5976–5980.
- Reiff, P. H. & Luhmann, J. G. 1986 In *Solar-wind-magnetosphere coupling* (ed. Y. Kamide & J. A. Slavin), pp. 453–476. Tokyo: Terra Scientifica.
- Reiff, P. H., Spiro, R. W., Wolf, R. A., Kamide, Y. & King, J. H. 1985 *J. geophys. Res.* **90**, 1318–1324.
- Richardson, I. G., Owen, C. J., Cowley, S. W. H., Galvin, A. B., Sanderson, T. R., Scholer, M., Slavin, J. A. & Zwickl, R. D. 1989 *J. geophys. Res.* (In the press.)
- Rishbeth, H., Smith, P. R., Cowley, S. W. H., Willis, D. M., van Eyken, A. P., Bromage, B. J. I. & Crothers, S. R. 1985 *Nature, Lond.* **318**, 451–452.
- Sandholt, P. E., Deehr, C. S., Egeland, A., Lybakk, B., Viereck, R. & Romick, G. J. 1986 *J. geophys. Res.* **91**, 10063–10079.
- Siscoe, G. L. & Huang, T. S. 1985 *J. geophys. Res.* **90**, 543–547.
- Southwood, D. J. 1987 *J. geophys. Res.* **92**, 3207–3217.
- Southwood, D. J., Saunders, M. A. & Farrugia, C. J. 1988 *Planet. Space Sci.* **36**, 503–508.
- Todd, H., Bromage, B. J. I., Cowley, S. W. H., Lockwood, M., van Eyken, A. P. & Willis, D. M. 1986 *Geophys. Res. Lett.* **13**, 909–912.
- Todd, H., Cowley, S. W. H., Etemadi, A., Bromage, B. J. I., Lockwood, M. & Willis, D. M. 1988*b* *J. atmos. terr. Phys.* **50**, 423–446.
- Todd, H., Cowley, S. W. H., Lockwood, M., Willis, D. M. & Lühr, H. 1988*a* *Planet. Space Sci.* **36**, 1415–1428.
- Waldock, J. A., Southwood, D. J., Freeman, M. P. & Lester, M. 1988 *J. geophys. Res.* **93**, 12883–12891.
- Willis, D. M., Lockwood, M., Cowley, S. W. H., van Eyken, A. P., Bromage, B. J. I., Rishbeth, H., Smith, P. R. & Crothers, S. R. 1986 *J. atmos. terr. Phys.* **48**, 987–1008.
- Wygant, J. R., Torbert, R. B. & Mozer, F. S. 1983 *J. geophys. Res.* **88**, 5727–5735.

### Discussion

M. SAUNDERS (*Imperial College, London, U.K.*). 1. A key characteristic of FTES seen at the magnetopause is that they are repetitive, recurring every 8–10 min. Is a similar periodicity present in events claimed to be the ionospheric signature of FTES?

2. Dr Lockwood showed a fine auroral picture taken by *Viking* which occurred during large IMF  $B_x$  conditions. Recent magnetohydrodynamic flow modelling indicates that such a field may develop a large southward component as it drapes over the magnetopause. Could it be that reconnection on this day is occurring equatorward, rather than poleward, of the cusp?

M. LOCKWOOD. 1. Yes, there is indeed a tendency for most of the reported observations of putative FTE signatures to show a recurrence with periods of about 5–10 min. In some cases, for example the ground-based optical data, this is one of the strongest similarities between the ionospheric and magnetopause data. One problem with magnetometer data is that some continuous pulsation phenomena (Pc5) have a similar period. Thus it can often be difficult to determine whether an observed sequence is a series of discrete impulsive events (with phase skips between them) or a continuous, damped wave train.

2. There is nothing in the Calgary group's uv images on that day to indicate that. All the changes occurred poleward of the poleward edge of the normal auroral oval, reflecting changes in the mantle and lobe, and there is no need to invoke draping effects.

R. J. MOFFETT (*Sheffield University, U.K.*). How does precipitation follow the polar-cap expansion? If there is no evidence, what is Dr Lockwood's view?

M. LOCKWOOD. There is no real data on that yet, only *in situ* data snapshots from passes of satellites. One of the exciting things that we hope to do with *Viking* and EISCAT is to observe the relationship continuously by using remote-sensing data (i.e. from the UV-imager with a non-scanning radar experiment like Polar). A plasma population is, of course, frozen on a given flux tube, so polar cap inflations and deflations due to the variations in reconnection rates will not on their own cause relative motions of the convection and precipitation boundaries. However, one reason that the flow reversal tends to sit within the precipitation region is the existence of any viscous-like interaction. Although having a low potential difference, this could be very important for high-latitude F-region modelling. The EISCAT data which I discussed do indicate that this interaction may be very variable on timescales of the order of an hour and greater, but I do not yet know by how much the separation of the two boundaries may fluctuate as a result.



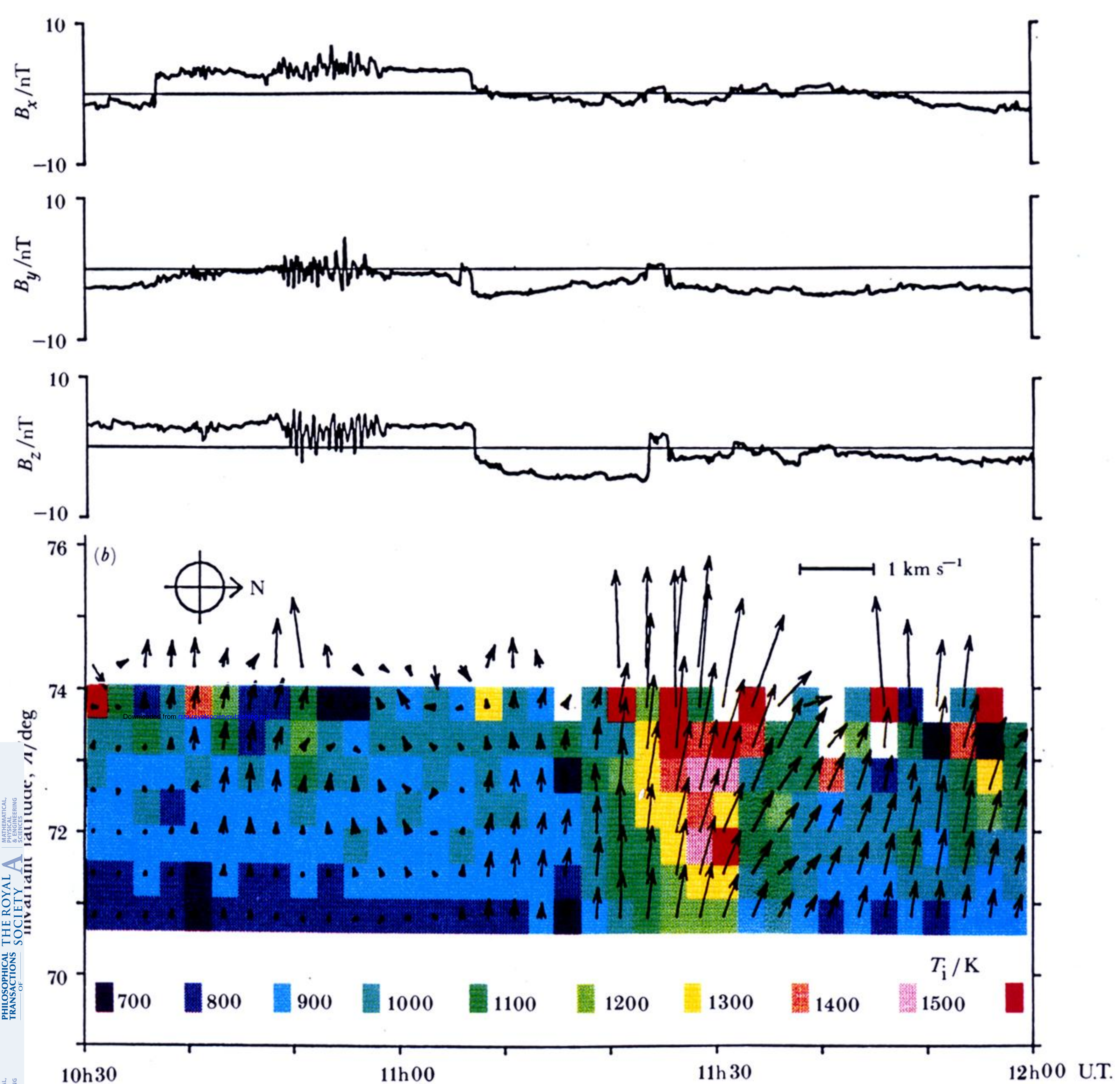


FIGURE 2. Example of an observed ionospheric response to a southward turning of the IMF (27 October 1984). (a) The sunward, downward and northward components of the IMF in GSM coordinates ( $B_x$ ,  $B_y$  and  $B_z$ , respectively), observed by *AMPTE-UKS* when located immediately sunward of the Earth's bow shock. (b) The simultaneous observations by the *EISCAT* radar. The flow vectors have been rotated through  $90^\circ$  to avoid congestion of the plot; hence northward flow is shown by vectors directed to the right of the figure and westward flow by vectors directed upward (i.e. the vectors are in the direction of the electric field). The vectors are superimposed on a colour plot of two-minute averages of the ion temperature,  $T_i$ . (From Willis *et al.* 1986.)



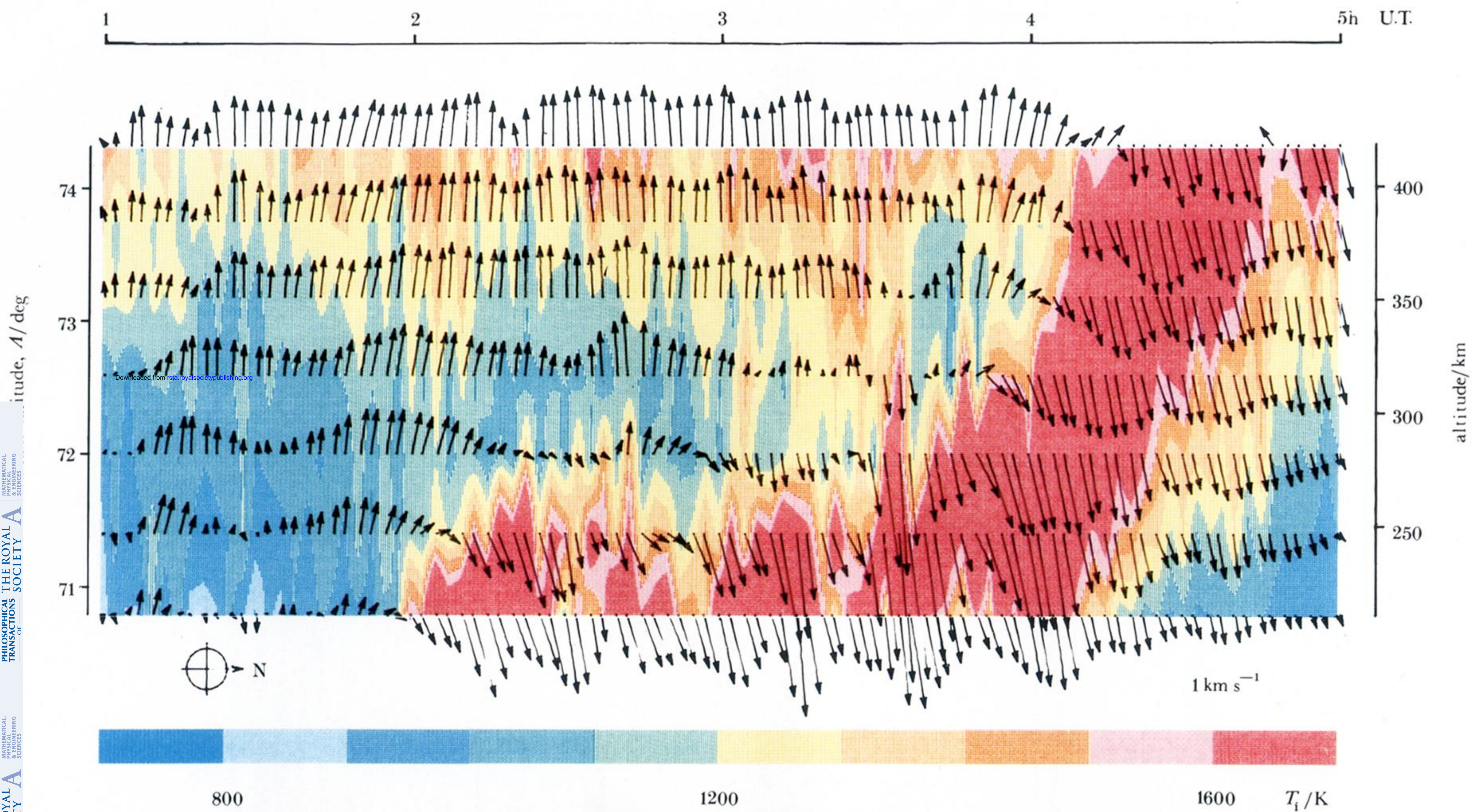


FIGURE 5. EISCAT observations of the polar cap boundary near dawn showing a polar cap contraction and evidence for viscous-like interaction across the magnetopause. The data presentation format is the same as that used in figure 2. A band of high ion temperature is seen immediately equatorward of the boundary which appears as a rotational reversal of the flow vectors from westward to eastward, through northward, and moves rapidly poleward across the field-of-view between 03h45 and 04h15 U.T.